Presented at the IRE National Convention, New York, N.Y., March 22-25, 1954

A HIGH EFFICIENCY - HIGH QUALITY AUDIO POWER AMPLIFIER

Alexander B. Bereskin
Professor of Electrical Engineering-University of Cincinnati
Consulting Engineer-The Baldwin Company
Cincinnati, Ohio

Summary. This paper deals with the design and performance of an audio power amplifier circuit which is capable of delivering more than 50 watts of audio power with very low harmonic and intermodulation distortion. The plate circuit efficiency approaches the ideal for class B operation. The amplifier has a very low output impedance and an unusual ability to stand up under abnormal operating conditions.

The circuit of Figure 1 is the result of a project to develop a large amount of good quality audio frequency power in a relatively small and inexpensive package.

In this circuit the 12AX7 acts as a combined amplifier, phase inverter, and direct coupled driver. The beam power output tubes operate class B_1. The output transformer has an electrostatically shielded feedback winding which is very closely coupled to the secondary. This feedback winding is connected in series with the input circuit.

The use of beam power tubes in class B_1 operation provides high efficiency and high power sensitivity. Both of these factors tend to reduce the cost and physical size required for a given power output.

Very high quality results from the fact that the circuit is capable of stable operation with large amounts of feedback. The circuit has been used with 36 db of feedback without showing any sign of instability, but the driving voltage required with this amount of feedback is excessive so that a compromise value of approximately 24 db is normally used.

A residual hum voltage 96 db below rated output was obtained with this circuit when it was operated with low ripple power supplies and a common filament supply for all tubes. One side of the filament supply was connected to ground and no effort was made to balance the tubes. An alternating current voltage of 42 volts inserted in series with the plate supply, or 9 volts inserted in series with the screen supply was necessary to bring the hum level in the output to 80 db below rated output.

Class B operation of the output stage imposes certain problems which were solved by special design features applied to the output transformer. Bifilar winding was used for the two primaries in order to reduce the leakage reactance which normally gives rise to the conduction transfer notch in this type of operation. Low leakage reactance between the primary and the secondary is obtained by sandwiching the secondary and the shielded feedback winding between the bifilar primaries which are wound in two sections.

The use of a bifilar primary introduces a high primary interwinding capacitance which tends to limit the high frequency power delivering capacity of the amplifier.

The primary interwinding capacitance is greatly reduced by winding the bifilar primary with a small spacing between the adjacent wires. A further 33 1/3 per cent reduction in this capacitance may be obtained by transposing the bifilar wires at each turn. A mechanism capable of transposing the bifilar winding at each turn has been developed and, while the winding speed in this case is slightly lower than that of an ordinary bifilar winding, it does not represent any particular difficulty not otherwise associated with bifilar windings. It is interesting to note that a random bifilar winding has only slightly more interwinding capacitance than the transposed bifilar winding and that this capacitance can further be reduced in the random bifilar case by winding a string along with the two wires.

Figure 2 is a schematic diagram of the output transformer used to make the tests discussed in the remainder of this paper. The nominal output impedance levels were intended to be 4, 8, and 16 ohms but the optimum levels obtained were 4.63, 9.25, and 18.5 ohms. An optimum value resistor was used on the 9.25 ohm tap on all of the succeeding tests.

Figure 3 shows the actual coil buildup that was used. The coil was designed to be used with two Moloney ME-31 grain oriented C cores. This diagram is drawn in proper vertical scale but the horizontal scale has been modified to show the relative positions of the windings without showing the true coil width.

The close couplings obtained between the primaries and the secondary and between the feedback winding and the 4 ohm section of the secondary are apparent from this diagram. This coil had a primary interwinding capacitance of .010 microfarads when it was vacuum impregnated with G. E. Type 9700 clear baking varnish and baked for the prescribed amount of time.

Figure 4 shows the performance of the

amplifier of Figure 1 used with the output transformer of Figure 3 and transformer coupled input to the circuit. In this Figure a harmonic distortion value of 2% was chosen as a limiting condition in determining the power delivering capacity of the amplifier. The amplifier is able to deliver more than 60 watts over most of the middle frequency region within the CCS plate dissipation rating of the tubes. The curve of plate circuit losses includes transformer losses which are estimated to be 4.5 watts for the full power condition at 60 cycles. The screen dissipation is slightly in excess of the rated CCS value. A reduction of 3 watts in the output power, over most of the range, brings the harmonic distortion below 1% and the screen dissipation safely below the rated CCS value. A maximum operating efficiency of 65.2% was obtained in the 500-1000 cycle region. If the transformer losses are considered to be a part of the tube output, the efficiency becomes 69% in this region.

Since transformer coupled input is not always convenient for amplifiers of this type a circuit including a preamplifier and power supply was developed and is shown in Figure 5. This circuit was designed to deliver 50 watts of high quality power over most of the middle frequency range. Since the output stage is very insensitive to ripple in the screen and plate supply circuits, very simple power supply filter circuits were adequate. Filter chokes were not necessary in either the plate or screen supply circuits. A single 5U4-G rectifier tube, operating within the manufacturer's ratings, was adequate to supply the power required by the plate circuits of the 1614 tubes. One 6X4 tube is used to supply the power required by the preamplifier and the screens of the 1614 tubes, while another 6X4 tube is used to supply the negative voltage required by the 12AX7 tube. The voltages indicated at various locations on the diagram are the measured no-load and full-load values.

The preamplifier consists of a two stage resistance-capacitance coupled amplifier with feedback between the second plate and the first cathode. This feedback provides good wave shape and low output impedance on the preamplifier. The preamplifier is coupled to the 12AX7 grid with a 1.25 microfarad capacitor and a modified Thordarson T20C51 choke. The modification consists in interleaving the laminations of this choke. A low dc resistance is necessary in this circuit because the 12AX7 has appreciable grid current when the grid voltage becomes more positive than -1 volt and this grid current must not be allowed to change the bias relations of the phase inverter. This coupling circuit has a low Q resonance between 10 and 15 cycles/sec.

Feedback from the secondary of the transformer is incorporated in a manner similar to that used before, but additional overall feedback has been incorporated from the 4.63 ohm tap to the first cathode in the preamplifier. It was found that a complex Bridged T network produced the best high frequency square wave response but that the square wave response was perfectly adequate when a simple 15 micromicrofarad capacitor was substituted in the overall feedback circuit. This capacitor has no effect on the low frequency response but reduces the tendency of the amplifier to ring slightly with sharp rise time square wave inputs. The photographs of Figure 6 show the manner in which the ringing, following the leading edge of a 10 watt - 5KC square wave, is modified by varying the value of this capacitor. The rise time of the leading edge is approximately 7.5 microseconds between the 10% and 90% points and the ringing frequency is approximately 100 K.C. The complete square wave response at 50, 500, and 5000 cycles/sec. and power levels of 10 and 40 watts is shown on Figure 7 together with the output of the square wave generator connected directly to the CRO. A greatly expanded view of the 40 watt - 5000 cycle/sec. case is shown on Figure 8. The gain control settings were not changed during these tests.

The results of tests made to determine the best balance between the various types of feedback are shown in Figure 9. In this figure curves 1 and 2 have inadequate feedback turns to correct for class B operation at low power levels. The Bridged T overall feedback network produced 6 db feedback at operating frequencies so that curve 1 is lower than curve 2 at high power levels. Curve 3 has much less low level distortion than curve 2 because of the additional feedback turns but it requires more drive from the preamplifier and therefore has higher distortion than curve 2 at high power levels. Curve 4 uses approximately 6 db additional feedback in the preamplifier and its distortion is quite satisfactory at both low and high power levels. The 15 micromicrofarad overall feedback has no effect at these frequencies. The values of feedback turns and preamplifier feedback resistance used in obtaining curve 4 represent a practical compromise between low input signal and low output distortion. Additional reduction in distortion could be obtained by increasing the number of turns on the feedback winding and reducing the value of the feedback resistor in the preamplifier. Both of these changes would increase the input voltage required to produce full output power. The conditions specified for curve 4 are the ones shown in the circuit diagram of Figure 5 and are the ones used in all succeeding tests. It can be seen from these curves that once the amplifier starts over-loading, the distortion increases very rapidly.

Figure 10 shows the curves of plate circuit losses (including transformer losses) and screen dissipation as the output power is varied. The plate circuit losses are less than the rated CCS values for all operating conditions. The screen dissipation becomes equal to the rated CCS value at the highest power levels shown but is less than the rated value at lower levels.

The 2% distortion power delivering capacity together with the corresponding plate circuit losses and screen dissipation are shown in Figure 11. The highest plate circuit efficiency, including transformer losses, occurred at 1000 cycles/sec. and was 69%. If the transformer losses are considered to be a part of the tube output, the plate efficiency becomes 72% at this frequency. The plate circuit losses are below the rated CCS value for the tubes alone and the screen dissipation is equal to the rated CCS value over most of the range. It should be emphasized that this curve represents the power delivering capacity of the amplifier and not the linearity of response with frequency variations. The frequency response characteristics, together with the power delivering capacity curve, plotted to a db scale, are shown in Figure 12. It can be seen from this diagram that as long as the operating level is below the 2% distortion curve the response is perfectly flat between 100 and 20,000 cycles/sec. Below 100 cycles/sec. the response rises slightly due to the series resonance in the impedance coupled circuit. The amount of this rise can be controlled by modifying the values of the coupling capacitor and choke. At low levels the response above 20,000 cycles/sec. depends on the amount of feedback capacitance used. The curve for $C_{fb} = 0$ is seen to rise to a maximum at about 85KC and then to drop off very rapidly. The curve for $C_{fb} = 15$ micromicrofarads is seen to be almost perfectly flat to 95KC after which it also drops off very rapidly. A curve for Gaussian response with a -3 db point at 75KC has also been shown for comparison purposes. It is seen that the ringing frequency of approximately 100KC corresponds closely to the region of maximum deviation of the actual response characteristic from the Gaussian response. This also shows why the use of $C_{fb} = 15$ micromicrofarads reduced the ringing amplitude obtained with a square wave input signal.

Figure 13 shows the results of an intermodulation distortion test using a 4:1 combination of 60 and 1500 cycles/sec. As is customary, the resulting distortion is plotted as a per cent of the smaller of the two signals. The values shown are acceptable up to at least 112% peak-to-peak equivalent input. An intermodulation distortion test was also performed for a 4:1 combination of 60 and 15,000 cycles/sec. and the results are shown in Figure 14. The purpose of this test was to find out if the high frequency roll off of the power delivering capacity had any appreciable effect on the intermodulation distortion. The values obtained in this test were slightly higher than those shown in Figure 13 but the performance is acceptable up to at least 105% peak-to-peak equivalent input.

Good transient response of a loudspeaker requires a low output impedance source. The manner in which the output impedance of this amplifier varies with frequency is shown in Figure 15. The output impedance remains relatively constant with frequency and is about 10% of the nominal impedance of the tap. This output impedance was relatively independent of the current used to make the test.

A short circuited secondary test was performed on the amplifier to determine its susceptibility to accidental damage. The results of this test are shown in Figure 16. The screen dissipation of the tube reaches 4.5 watts at relatively low signal levels but remains below 5 watts even with 120% of normal full load signal. With the same signal the plate circuit input approaches 120 watts. This is considerably greater than the rated value but the plate structure is quite rugged and capable of handling these powers for short periods of time. The screen grid of the tube is quite fragile compared to the plate structure so it is fortunate in this situation that it only has to handle about 70% of its rated dissipation. This amplifier was operated for 10 minutes at the highest signal condition shown on the graph. At the end of the ten minute period the short circuit was removed and the amplifier operated normally. No damage could be detected in any part of the amplifier or its tube complement.

The amplifier can also operate with full signal applied under open secondary conditions. The only noticeable change is that the output voltage rises by about ten per cent when the load is disconnected. This control is due to the close coupling used between the secondary and the feedback winding.

The residual hum in the complete amplifier is slightly greater than that measured in the basic amplifier with transformer coupled input. For the complete amplifier the residual 120 cycle hum is about 80 db below 50 watts. The residual 60 cycle hum is about 66 db below 50 watts. Due to its lower frequency, the 60 cycle hum is no more serious than the 120 cycle hum and both have been found to be completely negligible in most cases. The 60 cycle hum is picked up inductively by the unshielded modified T20C51 choke from the power transformer. If further reduction of the 60 cycle hum is desirable and the amplifier is operated remotely from other equipment, this choke can be oriented for minimum 60 cycle pickup. Approximately 20 db reduction has been obtained by this means but a clumsy mounting position was required for the choke. If the equipment is operated in proximity to other equipment whose relative position may change from time to time, a better solution would be to use a fully shielded choke. It should be emphasized however that in most cases further hum reduction is not necessary.

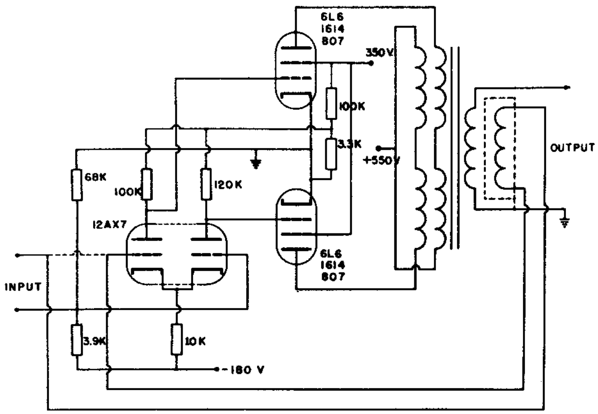

Fig. 1
Basic Bereskin power amplifier.

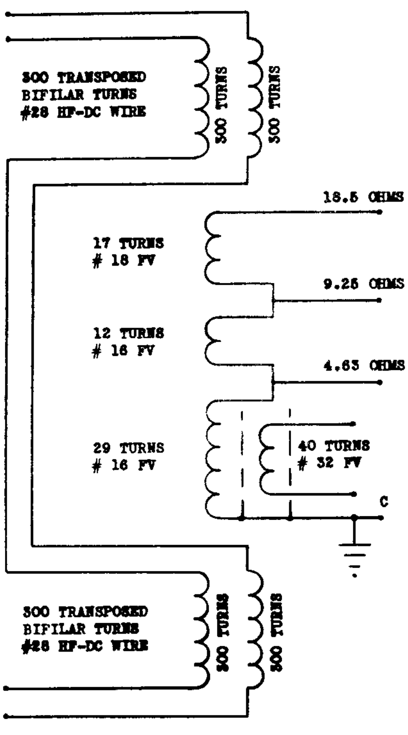

Fig. 2
Output transformer winding arrangement.

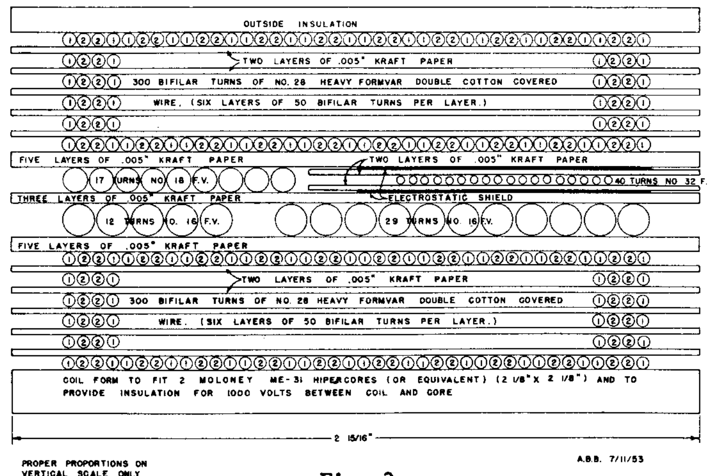

Fig. 3
Output transformer coil buildup.

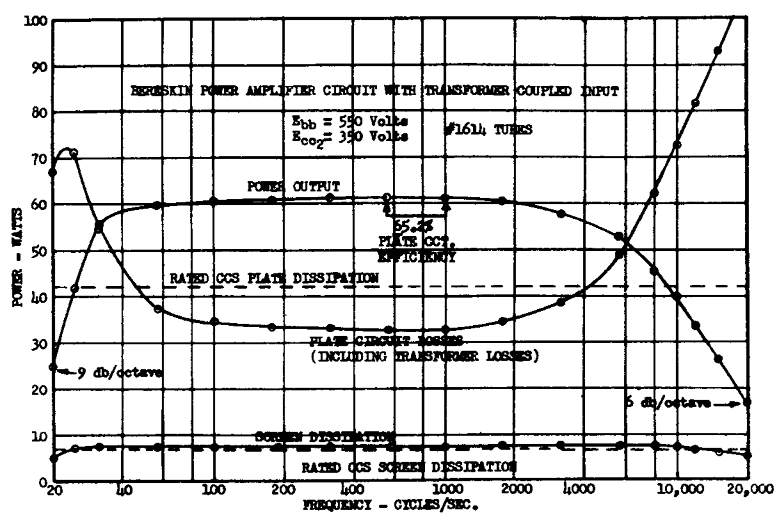

Fig. 4
2% distortion power relations for Bereskin power amplifier circuit with transformer coupled input.

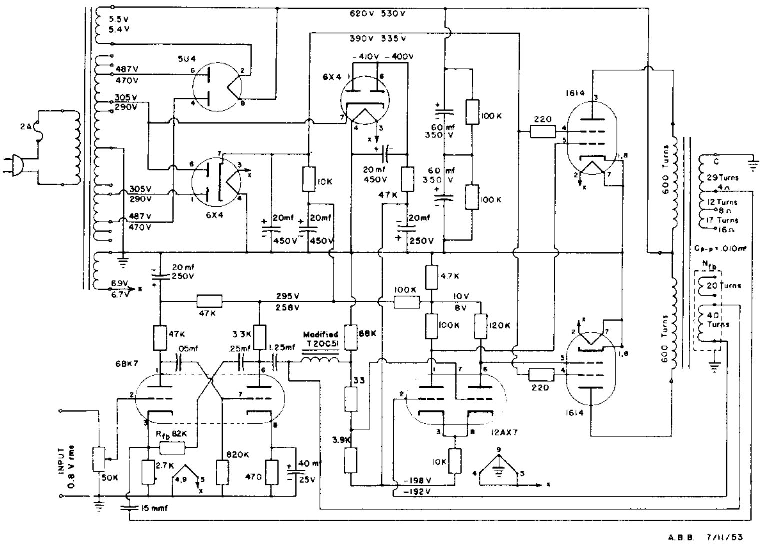

Fig. 5 (left)
Bereskin 50-watt 1614-tube power amplifier.

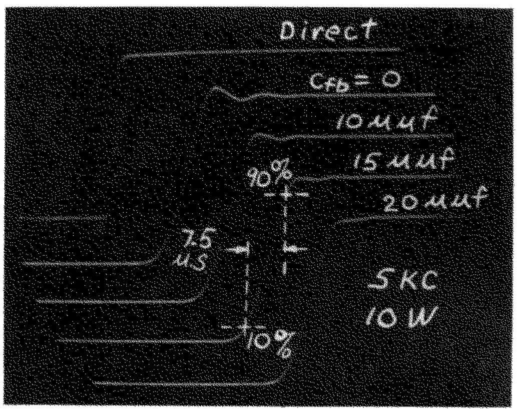

Fig. 6
Leading edge of 5-kc - 10-watt square wave.

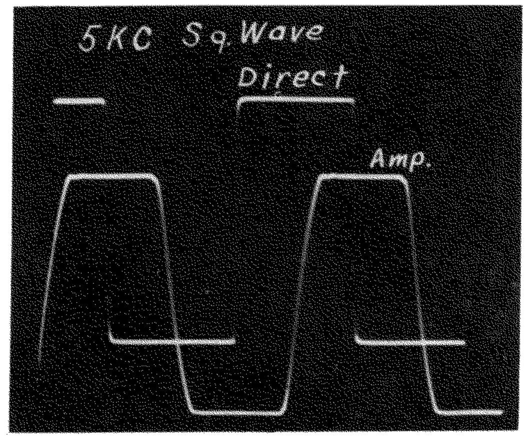

Fig. 8
Enlarged view of 40-watt
5-kc square wave response.

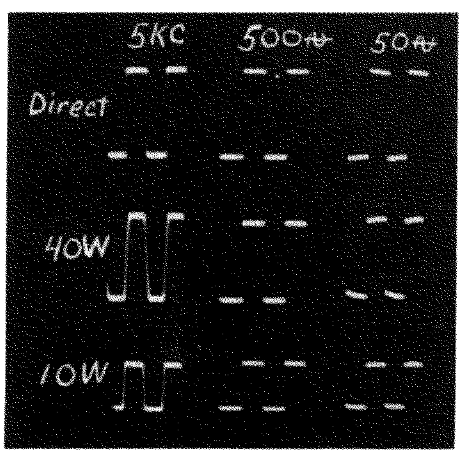

Fig. 7
Square wave response.

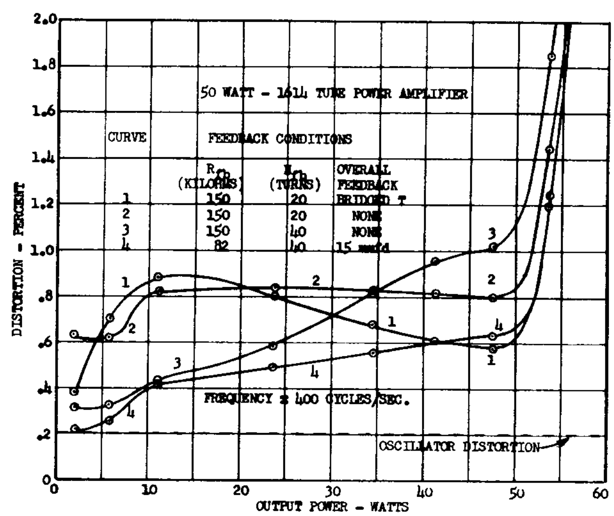

Fig. 9
Feedback - distortion characteristics.

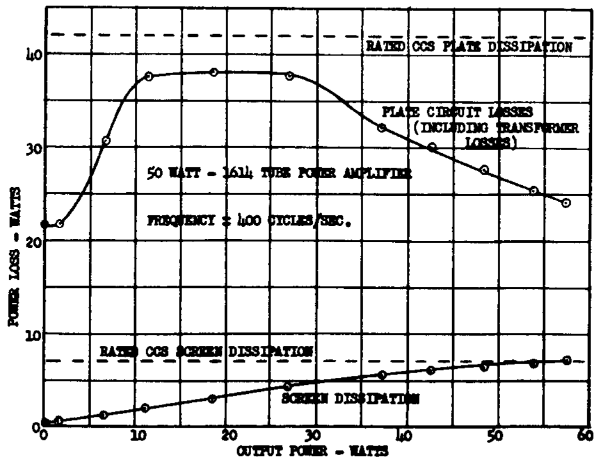

Fig. 10
Power loss characteristics.

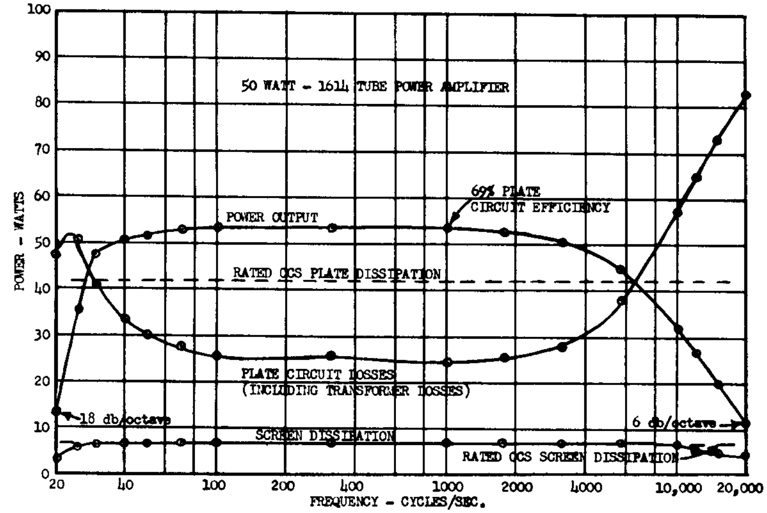

Fig. 11
2% distortion power relations.

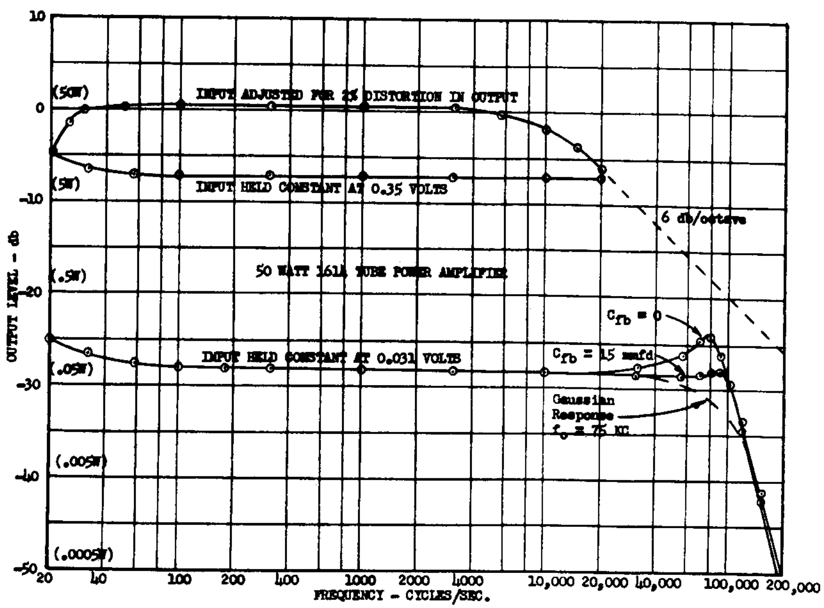

Fig. 12
Frequency response characteristics.

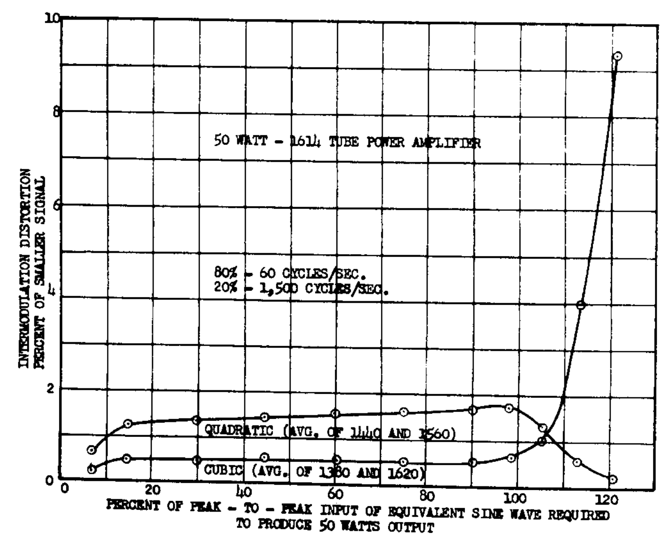

Fig. 13
Intermodulation distortion characteristics.

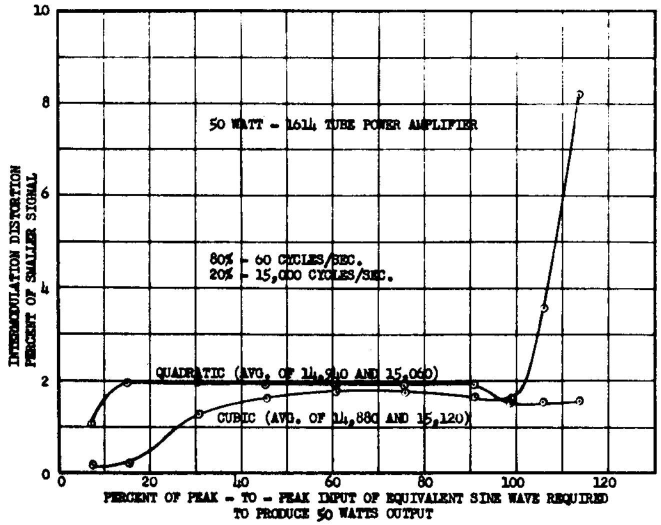

Fig. 14
Intermodulation distortion characteristics.

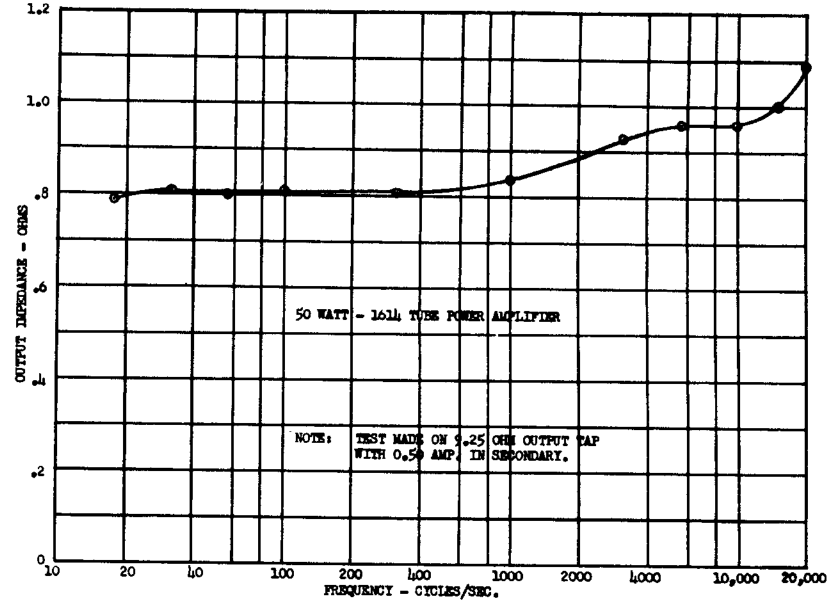

Fig. 15
Output impedance characteristic.

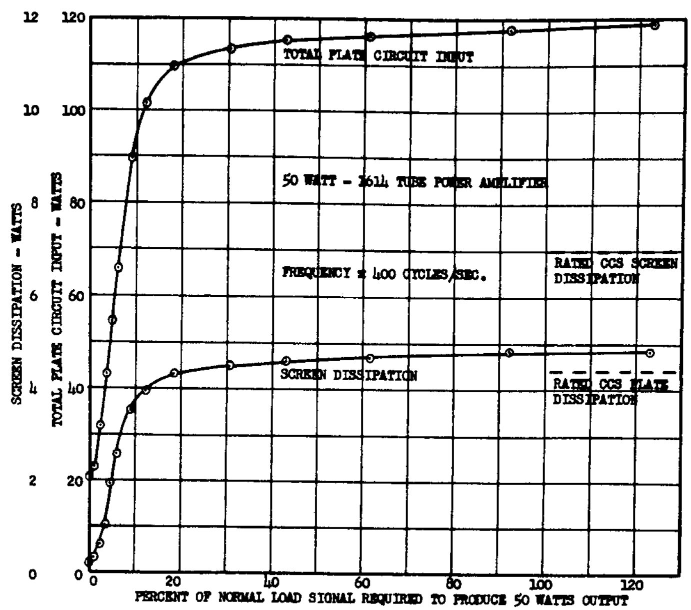

Fig. 16 (left)
Short circuited output - power relations.